Cerium Oxide Nanoparticles Protect Cardiac Progenitor Cells from Oxidative Stress
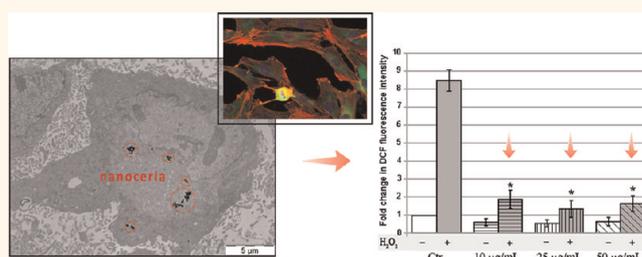
Francesca Pagliari,[†,‡,ǁ] Corrado Mandoli,[§,ǁ] Giancarlo Forte,[§] Eugenio Magnani,[†] Stefania Pagliari,[§] Giorgia Nardone,[†] Silvia Licoccia,[⊥] Marilena Minieri,[†] Paolo Di Nardo,[†,‡,*] and Enrico Traversa[⊥,*]

[†]Laboratory of Cellular and Molecular Cardiology, Department of Internal Medicine, University of Rome Tor Vergata, Rome, Italy, [‡]BioLink Institute, Link Campus University, Rome, Italy, [§]International Research Center for Materials Nanoarchitectonics (MANA), National Institute for Materials Science (NIMS), Tsukuba, Japan, and [⊥]NAST Centre & Department of Chemical Science and Technology, University of Rome Tor Vergata, Rome, Italy. [ǁ]These authors contributed equally to this work.

Recently, several nanomaterials currently used in different manufacturing domains have been scrutinized for their potential biomedical interest.[1−3] Among others, special attention has been paid to cerium oxide (CeO_2, ceria) nanoparticles (nanoceria) that are currently used in industrial applications, such as catalysis,[4] gas sensors,[5] UV filters,[6] and solid oxide fuel cells,[7] for their unique property to store and release oxygen.[8] This is due to the presence in ceria of a fraction of Ce ions in the Ce^{3+} valence state, simultaneously with Ce^{4+}, with oxygen vacancies compensating for the lower positive charge.[9] Nanoceria particles are more active with respect to the micrometer-sized counterpart because the defect concentration is increased at the surface,[10] as confirmed also by theoretical studies.[11] Therefore, ceria nanoparticles, where the larger surface area is associated with an increased number of oxygen vacancies and Ce^{3+} ions, showed enhanced catalytic properties[12] and antioxidant capability in living systems.[13−15] Moreover, a recent first-principles study showed that the vacancy concentration increases when ceria is exposed to water, which could be relevant in biological systems.[16] In fact, under physiological conditions, the cell oxidative metabolism produces reactive oxygen species (ROS), such as superoxide anion radical ($O_2^{•−}$), hydroxyl radical ($OH^{•−}$), singlet oxygen ($^1O_2$), and hydrogen peroxide (H_2O_2). ROS are unstable and highly reactive compounds able to extract electrons from cellular macromolecules to damage DNA and proteins and to modify membrane fatty acids, thus impairing major cell functions.[17] Consistently, ROS are implied in the pathogenesis of several diseases, such as cancer, Parkinson's and Alzheimer's

ABSTRACT

Cardiac progenitor cells (CPCs) are a promising autologous source of cells for cardiac regenerative medicine. However, CPC culture in vitro requires the presence of microenvironmental conditions (a complex array of bioactive substance concentration, mechanostructural factors, and physicochemical factors) closely mimicking the natural cell surrounding in vivo, including the capability to uphold reactive oxygen species (ROS) within physiological levels in vitro. Cerium oxide nanoparticles (nanoceria) are redox-active and could represent a potent tool to control the oxidative stress in isolated CPCs. Here, we report that 24 h exposure to 5, 10, and 50 μg/mL of nanoceria did not affect cell growth and function in cardiac progenitor cells, while being able to protect CPCs from H_2O_2-induced cytotoxicity for at least 7 days, indicating that nanoceria in an effective antioxidant. Therefore, these findings confirm the great potential of nanoceria for controlling ROS-induced cell damage.

KEYWORDS: cerium oxide · nanoparticles · nanoceria · cardiac progenitor cells · reactive oxygen species · oxidative stress

diseases, cardiovascular dysfunctions, inflammatory conditions, and aging.[18−21] On the other hand, intracellular antioxidative defense systems consisting of enzymatic (i.e., superoxide dismutase, SOD, and catalase) and non-enzymatic (i.e., vitamins C and E, thiols, and glutathione) components modulate ROS intracellular levels to regulate, as second messengers, cell growth and differentiation.[22]

Recent investigations have shown that ceria nanoparticles could scavenge ROS and act as a catalyst mimicking the activity

of SOD, the enzyme that catalyzes the dismutation of the superoxide radical anion in living cells,[23,24] and also possess a catalase-like activity with the ability to decompose H_2O_2 to O_2 and H_2O.[25] The analysis on two leukocyte cell lines, undergoing apoptosis *via* redox-dependent or independent mechanisms, revealed that the intracellular antioxidant effect is the direct cause of the anti-apoptotic and pro-survival effects of nanoceria *in vitro*: nanoceria only affects the redox-dependent apoptosis by means of Ce^{3+}/Ce^{4+} redox reactions.[26] Furthermore, when embedded into poly(lactic-*co*-glycolic acid) (PLGA) films, ceria nanoparticles enhance the adhesion and growth of adult cardiac progenitor cells (CPCs), driving their orientation into specific directions.[2]

Adult progenitor cells are precursors of all differentiated cells within a specific germ layer and are located in almost every district of the body, where they are responsible for the physiological cell turnover and tissue repair. Progenitor cells are surviving in special tiny regions of each tissue in which a critical environment (niche) is maintained by the surrounding cells. In these conditions, progenitor cells can self-renew or can be committed to a specific cell lineage.[27] In the myocardium, evidence for progenitor cell differentiation and cardiomyocyte turnover is given, but such processes appear modest and not sufficient to match the tissue needs, when an extensive heart damage occurs, as in myocardial infarction.[28,29] Nevertheless, many attempts at expanding cardiac progenitor cells *in vitro* have been undertaken to generate a sufficient number of suitable cells to set up clinically efficient and cost-effective treatments.[30] Progenitor cell culture *in vitro* requires the presence of microenvironmental conditions closely mimicking the natural cell surrounding *in vivo* (niche).[31,32] Among others, the antioxidant systems are fundamental to maintain ROS within physiological levels *in vitro*.[33] Ceria nanoparticles, either dispersed into the culture medium or embedded into the scaffold material, could represent a potent tool to control the oxidative stress in isolated cardiac progenitor cells.

The present study was designed to verify to which extent ceria nanoparticles could contribute to control the oxidative stress and growth of adult cardiac progenitor cells. The CeO_2 nanoparticles used were the same described in previous works,[2,26] having size in the 5–8 nm range. In particular, the effects induced by different amounts of nanoceria on Lin[neg]/Sca-1^{pos} CPCs challenged with a potent cell oxidant agent, H_2O_2, were investigated in terms of cyto-compatibility, internalization, and cell morphology and differentiation. Such cells are shown to be negative for the expression of mature hematopoietic cell lineage markers (Lin[neg]) but positive for the stem cell antigen-1, Sca-1 (Sca-1^{pos}), marker associated with multipotency and self-renewal in bone marrow and heart.[34,35]

RESULTS

Nanoceria Is Internalized by CPCs. In order to define the fate of nanoceria particles in CPCs after 7 day culture, ultrastructural analysis was performed to detect and localize the nanoparticles within the cells, after 24 h exposure to 10, 25, and 50 μg/mL CeO_2, as described in the Materials and Methods section. Figure 1 shows typical TEM micrographs of Lin[neg]/Sca-1^{pos} CPCs (hereafter referred to as CPCs) after treatment with 50 μg/mL CeO_2, as a representative example. Cerium oxide nanoparticles were uptaken by CPCs and were retained inside the cytoplasm as clusters of aggregated particles, not encapsulated by vesicular membranes.
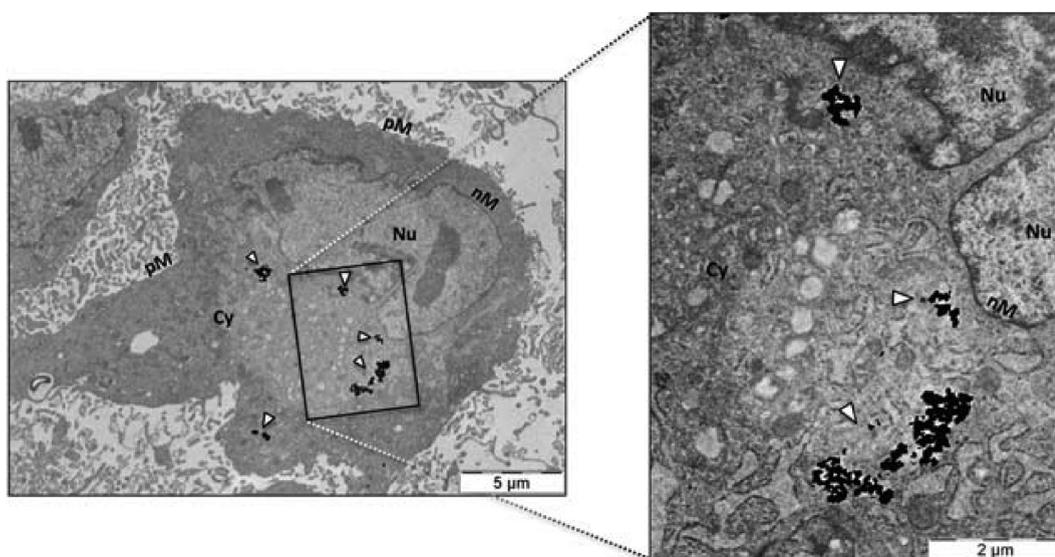

Figure 1. TEM micrographs of Sca-1^{pos} CPCs. The images illustrate the presence of clusters of ceria nanoparticles (white arrows) inside the cytoplasm, and they are representative of 50 μg/mL CeO_2 treatment after 7 days. Magnification: 3400× (left) and 11 500× (right); pM = plasma membrane, nM = nuclear membrane, Cy = cytoplasm, Nu = nucleus.
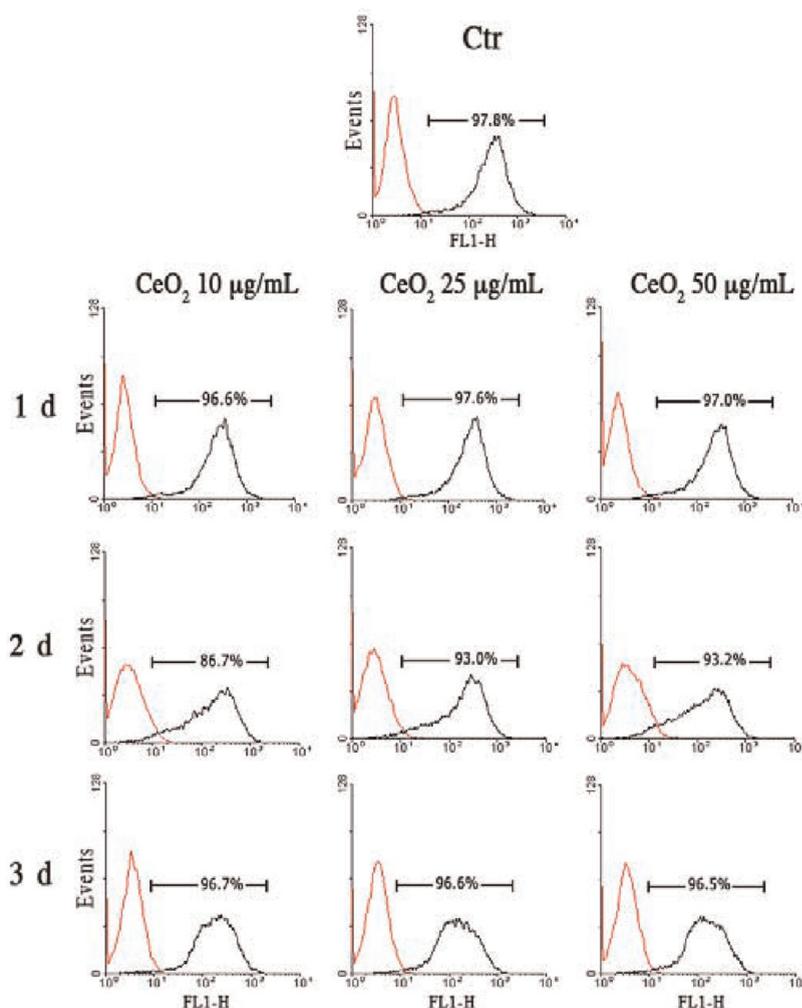
Figure 2. Sca-1 expression in CeO₂-treated CPCs analyzed by fluorescence activated cell sorter. CPCs preserved their stemness phenotype at all of the concentrations considered at 1, 3, and 7 days from nanoceria administration. Red curves represent the negative control obtained by incubating Sca-1^{pos} CPCs in the absence of anti-Sca-1 antibody. One representative image of Sca-1 expression in untreated CPCs (control, Ctr) at 24 h after the beginning of the experiment is given; same results were obtained at 3 and 7 days. The logarithm on the *X*-axis (FL1-H channel) represents the intensity of fluorescent signal; cell number is given on the *Y*-axis (Events). The data are representative of three independent experiments performed in the same conditions.

Nanoceria Does Not Alter CPC Phenotype and Growth. After 24 h ceria stimulus, the expression of the Sca-1 antigen was preserved in a high percentage of CPCs throughout the culture (Figure 2). Moreover, the immunofluorescence analysis indicated that the morphology of CeO₂-treated *versus* untreated CPCs was not modified, as shown by phalloidin staining of actin filaments (Figure 3a−d). In fact, treated CPCs exhibited a well-organized cytoskeleton and proper focal adhesions, as demonstrated by the typical expression of vinculin, a protein associated with cell−cell and cell−extracellular matrix (ECM) junctions. Furthermore, after a single initial nanoceria exposure, CPCs counts at 1, 3, and 7 days displayed a time−response but not a dose−response effect (Figure 3e).

CPC Differentiation Is Not Altered by Nanoceria Exposure. A hallmark of the stemness status is cell pluri/multipotency, that is, the ability to generate different cell phenotypes when progenitor cells are challenged with appropriate stimuli. To confirm their abided multipotency, nanoceria-treated CPCs were cultured in adipogenic or osteogenic media. After 10 days, lipid vacuoles or calcium deposits were detected in cell cytoplasm, thus demonstrating that the nanoceria treatment did not interfere with progenitor cell ability to proceed toward adipogenic (Figure 4a−d; scale bar = 20 μm) or osteoblastic (Figure 4e−h) lineages.

Furthermore, when directly cocultured with murine neonatal cardiomyocytes, nanoceria-treated Vybrant-red-labeled CPCs proceeded to cardiac commitment within 10 days. In fact, CPCs displayed an upregulated expression of GATA-4, the membrane translocation of connexin 43, and, more interestingly, the expression of the α-sarcomeric actinin (Figure 4i−t). Differentiation in nontreated CPCs cocultured with murine neonatal cardiomyocytes was as expected and already reported
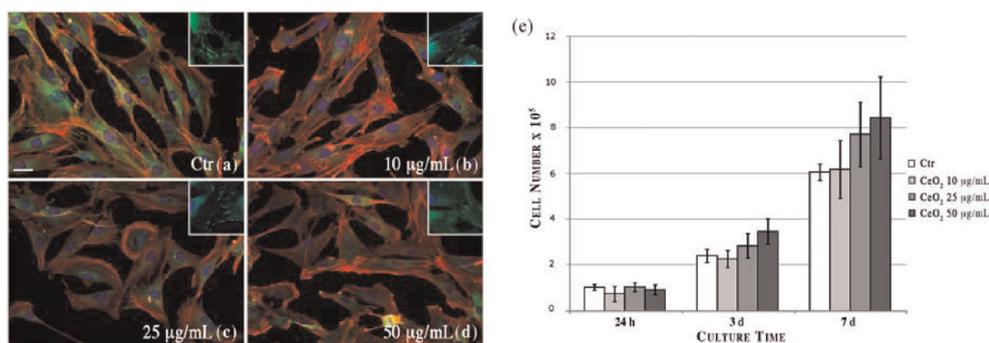
Figure 3. Effects of CeO$_2$ nanoparticles on CPC morphology and growth. CeO$_2$- untreated or treated cells [Ctr (a), 10 μg/mL (b), 25 μg/mL (c), and 50 μg/mL (d)] show a well-organized cytoskeleton and good cell−cell and cell−surface interactions, as demonstrated by staining F-actin filaments with rhodamine-labeled phalloidin (red) and antivinculin antibody (green), respectively. Insets at the top right: detail of cell focal adhesions. Similar results were obtained after 3 and 7 days in culture. Scale bar = 15 μm. (e) CPC growth in the presence of different CeO$_2$ concentrations. Cell number evaluated at 1, 3, and 7 days after 24 h exposure to nanoceria. The differences among treated and untreated (Ctr) cells were not significant ($p > 0.05$). The values are expressed as means $\pm$ SD of three independent measurements.
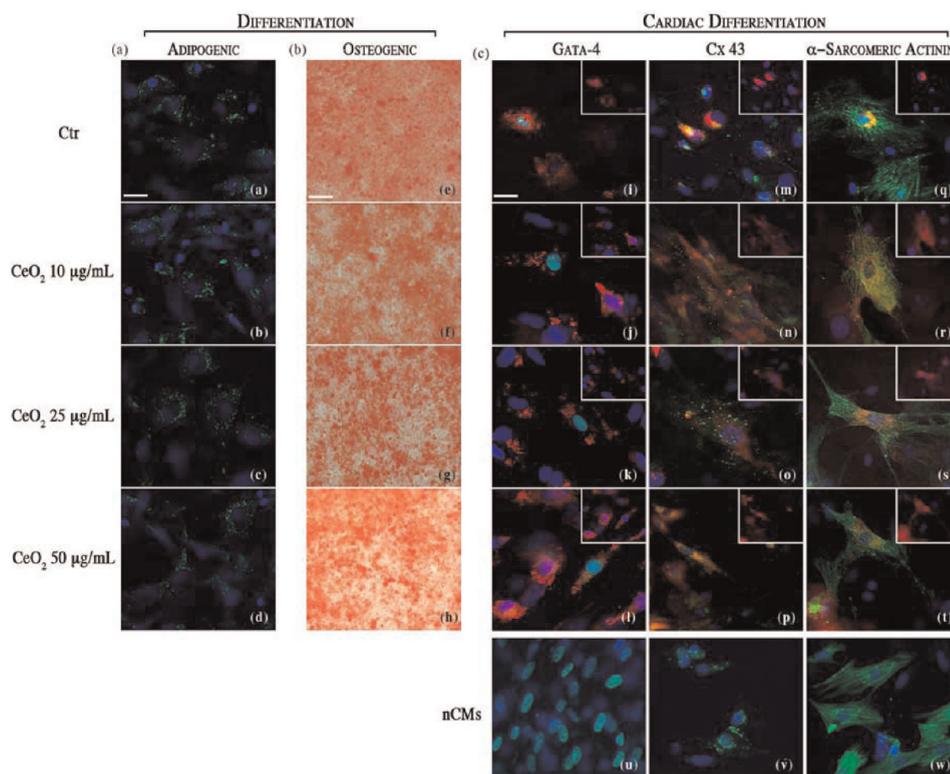

Figure 4. Sca-1^{pos} CPCs adipogenic, osteogenic, and cardiac differentiation in the presence of different concentrations of CeO$_2$. Adipogenic differentiation (a−d) was evidenced by the formation of intracytoplasmatic lipid vacuoles (green), stained with AdipoRed. Scale bar = 15 μm. Osteogenic differentiation (e−h) was demonstrated by calcium deposits (red) which were shown by Alizarin Red S staining. Scale bar = 150 μm. For cardiac differentiation (i−t), Sca-1^{pos} CPCs were pretreated with vital Vybrant dye (red) and put in coculture with nCMs for 10 days. Treated CPCs preserved their ability to acquire typical cardiac markers (GATA-4, Cx 43, and α-sarcomeric actinin, in green). Nontreated CPCs and nCMs (u−w) were used as positive controls. Nuclei were labeled with DAPI (blue). Scale bar = 15 μm.

previously[32] and not significantly different with respect to the CeO$_2$-treated CPCs (Figure 4u−w).

Nanoceria Protects CPCs from Oxidative Insults. The ceria antioxidant effects were assessed in CPCs exposed to ROS generation and oxidative stress by H$_2$O$_2$. As shown in Figure 5, no significant differences in ROS production were detectable in CPCs preincubated with nanoceria for 24 h, as compared to control, thus suggesting

that CeO$_2$ did not promote ROS generation. Instead, a significant decrease in the intensity of DCF fluorescence, indicating that the ROS content was attenuated, was observed when CPCs were challenged with H$_2$O$_2$, after 24 h pretreatment with 50 μg/mL nanoceria, but not with the smaller concentrations (10 and 25 μg/mL). By contrast, a significant decrease in CPC intracellular ROS levels was detectable when the effects of 25 and
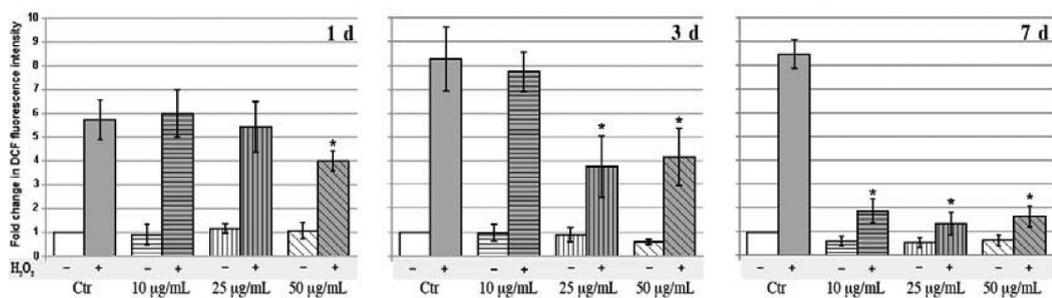
Figure 5. ROS production in Sca-1^{pos} CPCs exposed to H$_2$O$_2$. The results indicated a time-dependent decrease in ROS production when the cells were pretreated with different concentrations of CeO$_2$, as assessed by DCF fluorescence (*: H$_2$O$_2$-treated cells *vs* CeO$_2$–H$_2$O$_2$-treated cells). ROS levels in the control group were arbitrarily set at fluorescence value of 1. All data are expressed as means ± SD of three independent experiments and each repeated in triplicate. The relative SD of the samples has been calculated after normalization of the values compared to the mean values of the CeO$_2$ untreated control (negative) ($p < 0.05$).

50 μg/mL CeO$_2$ administered as single initial 24 h pulse were allowed to proceed for 3 days before the H$_2$O$_2$ stimulus. Moreover, a reduced ROS production was observed when H$_2$O$_2$ was added to the culture medium 7 days after the nanoceria pretreatment, independently from the nanoparticle dose (Figure 5).

DISCUSSION

Nanoparticles are actively scrutinized for their potential noxious effects in living systems[36−38] and also for some characteristics potentially exploitable for biotechnological and clinical purposes.[1,3,39,40] However, current knowledge is still unsystematic and restricted to particular aspects of nanoparticles' capability to induce toxic and pathological processes or to alter structure and function in different cell types.[41−43] Nevertheless, among nanoparticles, ceria is redox-active and has shown potential for antioxidant therapies controlling ROS levels.[44] This nanoceria characteristic could also be deployed to maintain ROS balance in progenitor cells used for reconstructing *in vitro* cardiac tissues.[45]

In this context, no study has been so far carried out to define nanoparticle effects on cardiac progenitor cell structure and function, to the best of our knowledge. Stem/progenitor cells are particularly sensitive to environmental factors,[46] and the presence of alien particles inside the cytoplasm or in the nearby extracellular space could cause major perturbations in their behavior and fate. Indeed, present findings demonstrated that CPCs resident into the heart were prone to uptake cerium oxide nanoparticles as aggregates, seemingly floating in the cytosol, while no evidence of encapsulation or particle translocation inside vesicles or organelles[44] was found by electron microscopy after 7 days from ceria administration. Furthermore, free-floating intracellular ceria nanoparticles did not alter the CPC cytoskeleton, as defined by F-actin filaments and DAPI-stained nuclei, and no apparent intracellular signs (nanoparticle encapsulation, *etc.*) were detectable that could suggest that nanoparticles could be removed or inactivated. As a matter of fact, after a single administration, CPCs underwent a stable and permanent ceria colonization that was not maintained by a continued nanoparticle supply from the extracellular compartment and did not provoke apparent cell structural damages.

The integrity of ceria-intruded CPCs was also confirmed by the preserved Sca-1 expression and multilineage potential. In fact, despite the persistent presence of ceria nanoparticles into the cytosol, CPCs retained the capability to multidifferentiate and, when properly cocultured with neonatal cardiac cells, to adopt the cardiomyocyte phenotype, as demonstrated by the expression of cardiac-specific proteins, such as the α-sarcomeric actinin in newly formed sarcomeres, GATA-4, a cardiac nuclear transcription factor, and connexin 43, a gap junction protein, which is necessary to establish cardiomyocyte electromechanical junctions. In addition, ceria did not affect CPC survival or growth *in vitro*. Finally, the nanoparticle inertness in interacting with CPC intracellular physicochemical mechanisms was confirmed by the ceria inability to modify basal ROS levels and to induce cytotoxicity, as described in other mammalian cell types.[47,48] Taken together, ceria nanoparticles uptaken during 24 h pulse persisted for the total length (7 days) of the experiments inside CPCs cultured in a standard medium deprived of nanoparticles; nonetheless, they did not induce apparent structural and functional cell modifications. However, in several cell types, nanoceria plays an antioxidant and antiapoptotic role related to the presence of Ce^{3+} ions.[13−15,26] Moreover, in a more recent *in vivo* study, a combination of nanoceria and sodium selenite improved diabetes-induced oxidative stress in a murine model of diabetes.[49] For CPCs, internalized ceria antioxidant effects emerged only when cells were exposed to an oxidative stress induced by H$_2$O$_2$ and were dose- and time-dependent. Following a 24 h single pulse, 50 μg/mL ceria nanoparticles displayed a time-dependent incrementing capability to decrease ROS levels by 30, 50, and 75% after 1, 3, and

7 days, respectively. Instead, pulses with smaller nanoparticle doses (10 and 25 μg/mL) needed a longer dose-related activation time to express their antioxidant capability. In fact, 25 μg/mL nanoceria antioxidant activity was displayed only after 3 days (50% reduction as compared with untreated cells) and was maximal at 7 days (-80%), while 10 μg/mL CeO$_2$ preloading attenuated ROS production (-70%) exclusively at 7 days.

These findings clearly demonstrated that uptaken ceria nanoparticles are a potent antioxidant agent and CeO$_2$ preloading attenuates ROS production over time to levels not significantly different from basal values in untreated cells. This observation is extremely relevant since no investigation before demonstrated that, after an unpredictable time interval, even low intracellular nanoparticle doses can induce effects undetectable by conventional, although sophisticated, analysis protocols. In stem cells, this possibility is particularly critical since ROS baseline levels and genomic instability are closely related, and the balance between ROS concentration and antioxidant agents is fundamental to preserve the cellular systems devoted to DNA repair[50] and the ROS key role in intracellular signaling.[22]

These findings are very promising for the use of nanoceria in regenerative medicine[51] since an adequate presence of ceria nanoparticles embedded into the scaffold or into cells could contribute, limiting the generation of ROS, to create the most favorable artificial microenvironment to maintain cardiac progenitor cells in optimal conditions during *in vitro* tissue growth. The results suggest that the effective nanoceria dose may be represented by the amount of uptaken nanoparticles, in fact after 24 h exposure, the extracellular nanoceria was removed by repeated washings and the protective effects occurred in the presence of cytosolic nanoparticles even 3 and 7 days after nanoceria removal. However, a proper dose has to be determined; otherwise, the delayed effects induced by low doses of ceria could be ineffective to adequately protect cells against an excess of ROS.

Another noteworthy finding is the long-term antioxidant action of nanoceria, unprecedented in the conventional antioxidant drugs,[26] which is persistent up to 7 days and only due to the nanoparticles uptaken from the cells, as confirmed by the untreated controls. We speculate that this could be related to a possible autoregenerative reactive cycle of cerium very likely activated *in vitro*,[44] thus allowing a continuous regeneration of the antioxidant activity, which could favor its activity over time with a single nanoparticle administration. Among the different hypotheses formulated to explain the ceria antioxidant mechanisms, as stated above, recent abiotic investigations suggested that nanoceria could have a SOD-like activity when a large Ce^{3+} fraction is present,[23,24] while a catalase-like activity is shown for nanoceria preparations with a large Ce^{4+} fraction.[25] The two redox reactions combined allow a continuous regeneration of the nanoceria antioxidant activity, potentially abating all noxious intracellular ROS *via* a self-regenerating mechanism, which could be enacted over time with a single nanoparticle administration.[44] The present findings might be the first experimental demonstration in a biological system of the nanoceria self-regenerating antioxidant mechanism. Nonetheless, the present time course experiments did not exclude that, in the long run, intracellular conditions, such as pH fluctuations or specific enzyme actions, could vary the surface Ce valence state, so contributing to both catalase and SOD mimetic activity.
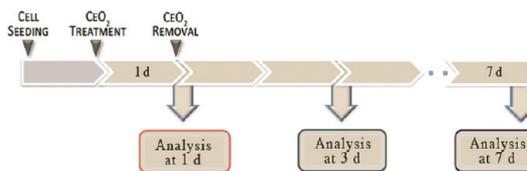
Present findings showed that time exposure to nanoparticles could be a major factor in ceria efficiency; in fact, nanoceria induced the same effects in ROS levels in time intervals inversely related to doses. Further studies are needed to fully understand this issue, although this could imply that a "threshold" must be reached in intracellular ceria physicochemical interactions before the antioxidant effects could emerge. In this respect, differences in nanoparticle synthesis techniques, size, shape and charge, dosage and exposure time, administration procedures, mechanisms of cellular uptake, and intracellular trafficking could be critical to induce ceria beneficial effects and to explain some conflicting results so far reported about ceria action in biological systems.[3,47,52] Moreover, the influence of culture medium components on nanoparticle charge and cell uptake and, thus, on their biological activity, also remains to be addressed.[53−55] However, all of these hypotheses need to be investigated more in-depth to exhaustively elucidate the time-dependent biological mechanisms supporting ceria antioxidant behavior.

The findings suggest another observation: the observed mechanism could imply that nanoparticles endowed with specific biological activities could remain silent inside cells for a long time interval, provided that they will not be degraded in biological fluids, and be eventually activated by slight intra- and/or extracellular environmental modifications. This phenomenon could envisage a new and unexpected scenario in the relationship between nanoparticles and cells. In fact, the interactions can be beneficial, triggering potential therapeutic effects like in the case of nanoceria, but can also be noxious with different nanoparticles. Due attention must be paid to assess the actuality of this perspective.

CONCLUSIONS

Unprecedented long-term protection from oxidative stresses, up to 7 days, of cardiac progenitor cells was demonstrated for internalized ceria nanoparticles after a 24 h initial treatment, without further contacts between CPCs and nanoceria. The internalized

nanoceria particles, which are inert with respect to CPC homeostasis and differentiation, remain apparently silent inside CPCs when compared with related controls and in the context of the present investigation and, in due course, act as a defense upon oxidative insults. The abatement of intracellular ROS may be due to a self-regenerating mechanism for nanoceria, involving redox cycles between the Ce^{3+} and Ce^{4+} oxidation states that react with superoxide and hydrogen peroxide, mimicking the role of the two key antioxidant enzymes, SOD and catalase. The present findings might be the first experimental demonstration in a biological system of this self-regenerating antioxidant

Scheme 1. Scheme of the experimental design used to test the CeO_2 antioxidant properties. Sca-1^{pos} CPCs were treated with different concentrations of CeO_2 nanoparticles (10, 25, and 50 μg/mL) for 24 h. Following a single CeO_2 exposure, cells were subjected to analysis at 1, 3, and 7 days.

mechanism, previously postulated for nanoceria from abiotic measurements.

MATERIALS AND METHODS

All experimental procedures and protocols used in this investigation were approved by the institutional Animal Care and Use Committee of the University of Rome Tor Vergata (Rome, Italy).

Isolation and Culture of Murine CPCs. CPCs were extracted from whole hearts derived from female B57/Bl mice (6 weeks old) housed under standard conditions. The myocardial tissue was delicately minced with a bistoury and incubated overnight at 4 °C with 0.05% trypsin in a solution of 0.02% EDTA in phosphate-buffered saline (PBS). Subsequently, trypsin inhibitor (Worthington Biochemical Corporation, Lakewood, NY, http://www.worthington-biochem.com) was used to block the enzymatic reaction, and tissue fragments were incubated in collagenase II (1500 U) in Leibovitz medium (Worthington Biochemical Corporation) for 30 min at 37 °C. Afterward, the fragments were centrifuged for 10 min at 800g, and the pellet was resuspended in DMEM (Dulbecco's modified Eagle's medium, Lonza, Walkersville, USA, Cat. No. BE12-614F) supplemented with 10% fetal bovine serum (FBS), 100 IU/mL penicillin, and 10 μg/mL streptomycin (Lonza; hereafter referred to as complete medium, http://bio.lonza.com/testpages-archive/cell-transfection-db/culture-media-database/#ext-comp-1003:tab_20:change), filtered through a 70 μm cell strainer (Falcon BD, Franklin Lakes, NJ, http://www.bdbiosciences.com), and incubated at 37 °C and 5% CO_2. After 24 h, the medium and the nonadhering fragments were removed and replaced with fresh medium. Cardiomyocytes were removed by changing the medium every day. After 10−15 days, fibroblastoid cells spontaneously migrated out from the fragments and reached confluence. These nonmyocytic cells (NMCs) were trypsinized and harvested.

NMC lineage positive (Lin[pos]) fractions were eliminated by a magnetic cell sorting protocol (Miltenyi Biotec GmbH, Bergisch Gladbach, Germany) in order to obtain the lineage negative fraction (Lin[neg]) of cell population. Briefly, cells were incubated with a cocktail of biotin-conjugated monoclonal antibodies (CD5, CD45R (B220), CD11b, anti-Ly-6G (Gr-1), 7-4, and Ter-119) and then separated by anti-biotin microbead-conjugated secondary antibody. The Lin[neg] fraction was resuspended in complete medium. Cell concentration was adjusted at 1.5×10^4 cells/cm² and expanded in culture.

Purification of Sca-1^{pos} CPCs. The Lin[neg]/Sca-1^{pos} fraction of CPCs (CPCs) was enriched by means of an immunomagnetic protocol. Briefly, the cells were detached from the dish surface by trypsin incubation, washed twice with PBS, and incubated with a microbead-conjugated antibody directed against the Sca-1 antigen. An aliquot of the purified cell subpopulations (Sca-1^{pos}, Sca-1^{neg}) was then stained with anti-Sca-1-FITC antibody (BD Pharmingen, Cat. No. 553335) for 20 min in ice cold PBS at 4 °C, centrifuged for 10 min at 800g, and resuspended in cold PBS. Green fluorescence of the samples was registered

using a FACScalibur flow cytometer (BD Biosciences, CA, USA). The results were analyzed using WinMDI 2.8 software.

CeO_2 Nanopowder Treatment. CeO_2 nanopowders, resuspended in ultrapure deionized H_2O, were produced and characterized as already described elsewhere.[3,8,27] The suspensions were freshly prepared, previously sonicated (Bandelin, Sonorex super RK 514 BH; Berlin, Germany) for 1 h, and immediately administered to the cells. CPCs (p7) were seeded at the concentration of 1.5×10^5/cm² in complete medium and maintained at 37 °C in 5% CO_2 atmosphere. After 24 h, the cells were untreated (negative control) or treated with 10, 25, or 50 μg/mL of CeO_2 nanopowder. Then, the cells were incubated for an additional 24 h, washed to remove the nanoceria powder, incubated with fresh medium, and analysis performed at various time intervals. Scheme 1 describes the experimental protocol used to assess the effects onto cardiac precursor cells of various nano-CeO_2 concentrations at 1, 3, and 7 days after starting the exposure to nanoparticles.

Transmission Electron Microscopy (TEM) Analysis. To investigate intracellular CeO_2 localization, CPCs were cultured in T25 flasks (Falcon BD) at the density of 2.0×10^5 cells/cm² in DMEM 10% FBS and treated with 10, 25, and 50 μg/mL nanoceria for 24 h at 37 °C in 5% CO_2 atmosphere. Afterward, cells were washed three times with PBS, incubated for an additional 7 days, and the medium was replaced by fresh medium at least every 2 days. Then, cells were detached by trypsin treatment, centrifuged, washed with PBS, and fixed overnight in 2.5% glutaraldehyde in 0.2 M phosphate buffer (pH = 7.2). The samples were postfixed with 1% osmium tetroxide (Merck, Germany) for 2 h and dehydrated in an ethanol series: 50, 75, 95 and 100% (×2) for 10 min. Subsequent passages in 100% alcohol and propylene oxide (1:1) and absolute propylene oxide were conducted. Then, the samples were embedded in growing resin (EPON 812, EMS USA) concentrations and placed in a 60 °C oven for 72 h. Finally, 30−50 μm sections were cut with an ultramicrotome, double stained with uranyl acetate−lead citrate, and examined in a Philips CM120 transmission electron microscope (TEM), operated at 60 kV and equipped with a Philips Megaview III video camera. Images were electronically captured by AnalySys 2.0 software and composed in an Adobe Photoshop CS4 format.

Immunofluorescence Analysis of CeO_2-Treated CPC Morphology and Cardiac Differentiation. CeO_2-treated CPCs were seeded at the concentration of 2×10^4 cells/cm² on chamber slides, washed in PBS, fixed in 4% paraformaldehyde (PFA) in PBS containing $CaCl_2$ for 30 min at 4 °C, and permeabilized with 0.1% Triton X-100. Cells were incubated with tetrarhodamine-conjugated phalloydine (Invitrogen Corp., Carlsbad, CA, http://www.invitrogen.com), antivinculin, anti-GATA-4, anticonnexin-43, and anti-α-sarcomeric actinin antibodies (Sigma-Aldrich, St. Louis, MO) in 1% PBS−BSA for 1 h at room temperature. The appropriate fluorophore-conjugated secondary antibodies were used. Nuclei were stained with 4′,6′-diamidino-2-phenylindole

(DAPI). Secondary antibodies in the absence of a specific primary antibody were used to exclude the occurrence of unspecific signals. The images were taken using a Leica DMRB microscope equipped with a digital camera.

Cell Counts. After 24 h ceria treatment, the first count (referred as day 1) was performed. Then, the cells were counted at days 3 and 7 after the initial nanoceria treatment. For cell counts, CPCs were detached by using a solution containing 0.05% trypsin in 0.02% EDTA. After stopping the reaction with complete medium, cells were centrifuged for 10 min at 800g. The pellet was resuspended in complete medium, and counts were performed by trypan blue exclusion method with Neubauer chamber. Each count was repeated at least three times.

Differentiation Protocols. Lin^{neg}/Sca-1^{pos} CeO$_2$-treated CPCs (p7) were seeded onto 35 mm dishes in complete medium. After 24 h, the medium was removed and the cells were cultured in standard adipogenic (Lonza, Cat. No PT3102B, http://bio.lonza.com/3018.html#ext-comp-1003:tab15:change)[56] or osteogenic (DMEM 10% supplemented with 50 μg/mL ascorbic acid, 10 mM β-glycerophosphate, and 10 nM dexamethasone; all from Sigma-Aldrich)[57] medium for 10 days.

Adipogenic Differentiation. Adipogenic differentiation was assessed by AdipoRed lipid assay reagent (Lonza, Cat. No PT-7009). Briefly, cells cultured in adipogenic medium were incubated for 20 min in AdipoRed solution, and the presence of lipid vacuoles was visualized under a fluorescence microscope.

Osteogenic Differentiation. Osteogenic differentiation was assessed by staining cells with Alizarin Red S for 20 min, and the production of calcium deposits was confirmed with light microscopy.

Cardiac Differentiation. We followed an *in vitro* cardiac differentiation protocol previously developed, using neonatal cardiomyocytes (nCMs) isolated from 1 to 3 day old neonatal murine hearts of C57/Bl6 mice.[33] For coculture experiments, nCM preparation was plated at a density of 5.0 × 10^4 cells/cm^2 onto precoated glass chamber slides (Nalgene, Nunc International). The day after, CPCs treated with different CeO$_2$ concentrations for 24 h were prestained with viable red fluorescent dye Vybrant DiI (Molecular Probes, Eugene, OR) following the manufacturer's specifications and seeded directly onto cardiomyocytes at a 1:5 ratio in complete medium. The medium was changed every other day throughout the entire experiment. Cells were cocultured for 10 days before being processed for immunofluorescence analysis. Control CPCs without pretreatment with CeO$_2$ were prepared in the same conditions and used as a control.

Intracellular ROS Induction and Determination. ROS were induced in 1.5 × 10^4 cells/cm^2 CPCs by 50 μM H$_2$O$_2$ treatment for 30 min in DMEM 10% serum after being exposed for 24 h to 10, 25, and 50 μg/mL of CeO$_2$. To quantify ROS production, the 2′,7′-dichlorfluorescein diacetate (DCFH-DA) method was used.[58] DCFH-DA is a membrane-permeant compound and, once inside the cell, it is deacetylated by endogenous esterases to form the nonfluorescent 2′,7′-dichlorfluorescein (DCFH). Next, DCFH is converted to fluorescent dichlorofluorescein (DCF) compound by the action of cellular oxidants. As a result, green fluorescence is emitted in response to ROS production and analyzed by flow cytometry. DCFH-DA (Sigma-Aldrich) was resuspended in dimethyl sulfoxide (DMSO, Sigma Aldrich). Briefly, cells were incubated with DCFH-DA solution at a final concentration of 6 μM in DMEM without serum for 30 min at 37 °C in 5% CO$_2$ atmosphere. Afterward, cells were rinsed twice with PBS, collected with trypsin-EDTA solution, centrifuged at 800g for 7 min, and the supernatant was discarded. The pellets were suspended with PBS, and 1 × 10^4 events were registered for each sample by using the FACScalibur flow cytometer. ROS level was expressed as the ratio mean intensity of sample/mean intensity of control cells. The data were analyzed by WinMDI 2.8 software.

Statistical Analysis. The results are shown as mean ± standard deviation (SD) as derived by unpaired t test. The values are considered significantly different when $p < 0.05$.

Conflict of Interest: The authors declare no competing financial interest.

REFERENCES AND NOTES

1. Han, G.; Ghosh, P.; De, M.; Rotello, V. M. Drug and Gene Delivery Using Gold Nanoparticles. *NanoBiotechnology* **2007**, *3*, 40–45.

2. Mandoli, C.; Pagliari, F.; Pagliari, S.; Forte, G.; Di Nardo, P.; Licoccia, S.; Traversa, E. Stem Cell Aligned Growth Induced by CeO$_2$ Nanoparticles in PLGA Scaffolds with Improved Bioactivity for Regenerative Medicine. *Adv. Funct. Mater.* **2010**, *20*, 1617–1624.

3. Karakoti, A.; Singh, S.; Dowding, J. M.; Seal, S.; Self, W. T. Redox-Active Radical Scavenging Nanomaterials. *Chem. Soc. Rev.* **2010**, *39*, 4422–4432.

4. Trovarelli, A. Catalytic Properties of Ceria and CeO$_2$-Containing Materials. *Catal. Rev.* **1996**, *38*, 439–520.

5. Jasinski, P.; Suzuki, T.; Anderson, H. U. Nanocrystalline Undoped Ceria Oxygen Sensor. *Sens. Actuators, B* **2003**, *95*, 73–77.

6. El-Toni, A. M.; Yin, S.; Sato, T. Enhancement of Calcia Doped Ceria Nanoparticles Performance as UV Shielding Material. *Adv. Sci. Technol.* **2006**, *45*, 673–678.

7. Esposito, V.; Traversa, E. Design of Electroceramics for Solid Oxide Fuel Cell Applications: Playing with Ceria. *J. Am. Ceram. Soc.* **2008**, *91*, 1037–1051.

8. Hailstone, R. K.; DiFrancesco, A. G.; Leong, J. G.; Allston, T. D.; Reed, K. J. A Study of Lattice Expansion in CeO$_2$ Nanoparticles by Transmission Electron Microscopy. *J. Phys. Chem. C* **2009**, *113*, 15155–15159.

9. Zhang, F.; Wang, P.; Koberstein, J.; Khalid, S.; Chan, S. W. Cerium Oxidation State in Ceria Nanoparticles Studied with X-ray Photoelectron Spectroscopy and Absorption Near Edge Spectroscopy. *Surf. Sci.* **2004**, *563*, 74–82.

10. Migani, A; Vayssilov, G. N.; Bromley, S. T.; Illas, F.; Neyman, K. M. Greatly Facilitated Oxygen Vacancy Formation in Ceria Nanocrystallites. *Chem. Commun.* **2010**, *46*, 5936–5938.

11. Esch, F.; Fabris, S.; Zhou, L.; Montini, T.; Africh, C.; Fornasiero, P.; Comelli, G.; Rosei, R. Electron Localization Determines Defect Formation on Ceria Substrates. *Science* **2005**, *309*, 752–755.

12. Campbell, T. C.; Peden, C. H. Oxygen Vacancies and Catalysis on Ceria Surfaces. *Science* **2005**, *309*, 713–714.

13. Chen, J.; Patil, S.; Seal, S.; McGinnis, J. F. Rare Earth Nanoparticles Prevent Retinal Degeneration Induced by Intracellular Peroxides. *Nat. Nanotechnol.* **2006**, *1*, 142–150.

14. Tarnuzzer, R. W.; Colon, J.; Patil, S.; Seal, S. Vacancy Engineered Ceria Nanostructures for Protection from Radiation-Induced Cellular Damage. *Nano Lett.* **2005**, *5*, 2573–2577.

15. Das, M.; Patil, S.; Bhargava, N.; Kang, J. F.; Riedel, L. M.; Seal, S.; Hickman, J. J. Auto-catalytic Ceria Nanoparticles Offer Neuroprotection to Adult Rat Spinal Cord Neurons. *Biomaterials* **2007**, *28*, 1918–1925.

16. Fronzi, M.; Piccinin, S.; Delley, B.; Traversa, E.; Stampfl, C. Water Adsorption on the Stoichiometric and Reduced CeO$_2$(111) Surface: A First-Principles Investigation. *Phys. Chem. Chem. Phys.* **2009**, *11*, 9188–9199.

17. Kohen, R.; Nyska, A. Oxidation of Biological Systems: Oxidative Stress Phenomena, Antioxidants, Redox Reactions, and Methods for Their Quantification. *Toxicol. Pathol.* **2002**, *30*, 620–650.

18. Kumar, B.; Koul, S.; Khandrika, L.; Meacham, R. B.; Koul, H. K. Oxidative Stress Is Inherent in Prostate Cancer Cells and Is Required for Aggressive Phenotype. *Cancer Res.* **2008**, *68*, 1777–1785.

19. Emerit, J.; Edeas, M.; Bricaire, F. Neurodegenerative Diseases and Oxidative Stress. *Biomed. Pharmacother.* **2004**, *58*, 39–46.

20. Misra, M. K.; Sarwat, M.; Bhakuni, P.; Tuteja, R.; Tuteja, N. Oxidative Stress and Ischemic Myocardial Syndromes. *Med. Sci. Monit.* **2009**, *15*, 209–219.

21. Finkel, T.; Holbrook, N. J. Oxidants, Oxidative Stress and the Biology of Ageing. *Nature* **2000**, *408*, 239–247.

22. Sauer, H.; Wartenberg, M.; Hescheler, J. Reactive Oxygen Species as Intracellular Messengers during Cell Growth and Differentiation. *Cell. Physiol. Biochem.* **2001**, *11*, 173–186.

23. Korsvik, C.; Patil, S.; Seal, S.; Self, W. T. Superoxide Dismutase Mimetic Properties Exhibited by Vacancy Engineered Ceria Nanoparticles. *Chem. Commun.* **2007**, *14*, 1056–1058.

24. Heckert, E. G.; Karakoti, A. S.; Seal, S.; Self, W. T. The Role of Cerium Redox State in the SOD Mimetic Activity of Nanoceria. *Biomaterials* **2008**, *29*, 2705–2709.

25. Pirmohamed, T.; Dowding, J. M.; Singh, S.; Wasserman, B.; Heckert, E.; Karakoti, A. S.; King, J. E.; Seal, S.; Self, W. T. Nanoceria Exhibit Redox State-Dependent Catalase Mimetic Activity. *Chem. Commun.* **2010**, *46*, 2736–2738.

26. Celardo, I.; De Nicola, M.; Mandoli, C.; Pedersen, J. Z.; Traversa, E.; Ghibelli, L. Ce^{3+} Ions Determine Redox-Dependent Anti-apoptotic Effect of Cerium Oxide Nanoparticles. *ACS Nano* **2011**, *5*, 4537–4549.

27. Beltrami, A. P.; Cesselli, D.; Bergamin, N.; Marcon, P.; Rigo, S.; Puppato, E.; D'Aurizio, F.; Verardo, R.; Piazza, S.; Pignatelli, A.; *et al.* Multipotent Cells Can Be Generated *in Vitro* from Several Adult Human Organs (Heart, Liver, and Bone Marrow). *Blood* **2007**, *110*, 3438–3446.

28. Urbanek, K.; Torella, D.; Sheikh, F.; De Angelis, A.; Nurzynska, D.; Silvestri, F.; Beltrami, C. A.; Bussani, R.; Beltrami, A. P.; Quaini, F.; *et al.* Myocardial Regeneration by Activation of Multipotent Cardiac Stem Cells in Ischemic Heart Failure. *Proc. Natl. Acad. Sci. U.S.A.* **2005**, *102*, 8692–8697.

29. Bergmann, O.; Bhardwaj, R. D.; Bernard, S.; Zdunek, S.; Barnabé-Heider, F.; Walsh, S.; Zupicich, J.; Alkass, K.; Buchholz, B. A.; Druid, H.; *et al.* Evidence for Cardiomyocyte Renewal in Humans. *Science* **2009**, *324*, 98–102.

30. Davis, D. R.; Kizana, E.; Terrovitis, J.; Barth, A. S.; Zhang, Y.; Smith, R. R.; Miake, J.; Marbán, E. Isolation and Expansion of Functionally-Competent Cardiac Progenitor Cells Directly from Heart Biopsies. *J. Mol. Cell. Cardiol.* **2010**, *49*, 312–321.

31. Forte, G.; Carotenuto, F.; Pagliari, F.; Pagliari, S.; Cossa, P.; Fiaccavento, R.; Ahluwalia, A.; Vozzi, G.; Vinci, B.; Serafino, A.; *et al.* Criticality of the Biological and Physical Stimuli Array Inducing Resident Cardiac Stem Cell Determination. *Stem Cells* **2008**, *26*, 2093–2013.

32. Pagliari, S.; Vilela-Silva, A. C.; Forte, G.; Pagliari, F.; Mandoli, C.; Vozzi, G.; Pietronave, S.; Prat, M.; Licoccia, S.; Ahluwalia, A.; *et al.* Cooperation of Biological and Mechanical Signals in Cardiac Progenitor Cell Differentiation. *Adv. Mater.* **2011**, *23*, 514–518.

33. Matés, J. M. Effects of Antioxidant Enzymes in the Molecular Control of Reactive Oxygen Species Toxicology. *Toxicology* **2000**, *153*, 83–104.

34. Matsuura, K.; Nagai, T.; Nishigaki, N.; Oyama, T.; Nishi, J.; Wada, H.; Sano, M.; Toko, H.; Akazawa, H.; Sato, T.; *et al.* Adult Cardiac Sca-1-Positive Cells Differentiate into Beating Cardiomyocytes. *J. Biol. Chem.* **2003**, *279*, 11384–11391.

35. Tateishi, K; Ashihara, E.; Takehara, N.; Nomura, T.; Honsho, S.; Nakagami, T.; Morikawa, S.; Takahashi, T.; Ueyama, T.; Matsubara, H.; *et al.* Clonally Amplified Cardiac Stem Cells Are Regulated by Sca-1 Signaling for Efficient Cardiovascular Regeneration. *J. Cell. Sci.* **2007**, *15*, 1791–1800.

36. Brunner, T. J.; Wick, P.; Manser, P.; Spohn, P.; Grass, R. N.; Limbach, L. K.; Bruinink, A.; Stark, W. J. *In Vitro* Cytotoxicity of Oxide Nanoparticles: Comparison to Asbestos, Silica, and the Effect of Particle Solubility. *Environ. Sci. Technol.* **2006**, *40*, 4374–4381.

37. Gojova, A.; Guo, B.; Kota, R. S.; Rutledge, J. C.; Kennedy, I. M.; Barakat, A. I. Induction of Inflammation in Vascular Endothelial Cells by Metal Oxide Nanoparticles: Effect of Particle Composition. *Environ. Health Perspect.* **2007**, *115*, 403–409.

38. Jawad, H.; Boccaccini, A. R.; Ali, N. N.; Harding, S. Assessment of Cellular Toxicity of TiO$_2$ Nanoparticles for Cardiac Tissue Engineering Applications. *Nanotoxicology* **2011**, *5*, 372–380.

39. Moghimi, S. M.; Peer, D.; Langer, R. Reshaping the Future of Nanopharmaceuticals: *Ad Iudicium*. *ACS Nano* **2011**, *5*, 8454–8458.

40. Au, K. W.; Liao, S. Y.; Lee, Y. K.; Lai, W. H.; Ng, K. M.; Chan, Y. C.; Yip, M. C.; Ho, C. Y.; Wu, E. X.; Li, R. A.; *et al.* Effects of Iron Oxide Nanoparticles on Cardiac Differentiation of Embryonic Stem Cells. *Biochem. Biophys. Res. Commun.* **2009**, *379*, 898–903.

41. Hess, H.; Tseng, Y. Active Intracellular Transport of Nanoparticles: Opportunity or Threat?. *ACS Nano* **2007**, *1*, 390–392.

42. Kocbek, P.; Teskac, K.; Kreft, M. E.; Kristl, J. Toxicological Aspects of Long-Term Treatment of Keratinocytes with ZnO and TiO$_2$ Nanoparticles. *Small* **2010**, *6*, 1908–1917.

43. Dobrovolskaia, M. A.; McNeil, S. E. Immunological Properties of Engineered Nanomaterials. *Nat. Nanotechnol.* **2007**, *2*, 469–478.

44. Celardo, I.; Pedersen, J. Z.; Traversa, E.; Ghibelli, L. Pharmacological Potential of Cerium Oxide Nanoparticles. *Nanoscale* **2011**, *3*, 1411–1420.

45. Forte, G.; Pietronave, S.; Nardone, G.; Zamperone, A.; Magnani, E.; Pagliari, S.; Pagliari, F.; Giacinti, C.; Nicoletti, C.; Musarò, A.; *et al.* Human Cardiac Progenitor Cell Grafts as Unrestricted Source of Supernumerary Cardiac Cells in Healthy Murine Hearts. *Stem Cells* **2011**, *29*, 2051–2061.

46. Di Nardo, P.; Forte, G.; Ahluwalia, A.; Minieri, M. Cardiac Progenitor Cells: Potency and Control. *J. Cell. Physiol.* **2010**, *224*, 590–600.

47. Park, E. J.; Choi, J.; Park, Y. K.; Park, K. Oxidative Stress Induced by Cerium Oxide Nanoparticles in Cultured BEAS-2B Cells. *Toxicology* **2008**, *245*, 90–100.

48. Gojova, A.; Lee, J. T.; Jung, H. S.; Guo, B.; Barakat, A. I.; Kennedy, I. M. Effect of Cerium Oxide Nanoparticles on Inflammation in Vascular Endothelial Cells. *Inhal. Toxicol.* **2009**, *21*, 123–130.

49. Pourkhalili, N.; Hosseini, A.; Nili-Ahmadabadi, A.; Hassani, S.; Pakzad, M.; Baeeri, M.; Mohammadirad, A.; Abdollahi, M. Biochemical and Cellular Evidence of the Benefit of Combination of Cerium Oxide Nanoparticles and Selenium to Diabetic Rats. *World J. Diabetes* **2011**, *2*, 204–210.

50. Li, T. S.; Marbán, E. Physiological Levels of Reactive Oxygen Species Are Required To Maintain Genomic Stability in Stem Cells. *Stem Cells* **2010**, *28*, 1178–1185.

51. Karakoti, A.; Tsigkou, O.; Yue, S.; Lee, P. D.; Stevens, M. M.; Jones, J. R.; Seal, S. Rare Earth Oxides as Nanoadditives in 3-D Nanocomposite Scaffolds for Bone Regeneration. *J. Mater. Chem.* **2010**, *20*, 8912–8919.

52. Hirst, S. M.; Karakoti, A. S.; Tyler, R. D.; Sriranganathan, N.; Seal, S.; Reilly, C. M. Anti-inflammatory Properties of Cerium Oxide Nanoparticles. *Small* **2009**, *5*, 2848–2856.

53. Lynch, I.; Salvati, A.; Dawson, K. A. Protein−Nanoparticle Interactions: What Does the Cell See?. *Nat. Nanotechnol.* **2009**, *4*, 546–547.

54. Patil, S.; Sandberg, A.; Heckert, E.; Self, W.; Seal, S. Protein Adsorption and Cellular Uptake of Cerium Oxide Nanoparticles as a Function of Zeta Potential. *Biomaterials* **2007**, *28*, 4600–4607.

55. Limbach, L. K.; Li, Y.; Grass, R. N.; Brunner, T. J.; Hintermann, M. A.; Muller, M.; Gunther, D.; Stark, W. J. Oxide Nanoparticle Uptake in Human Lung Fibroblasts: Effects of Particle Size, Agglomeration, and Diffusion at Low Concentrations. *Environ. Sci. Technol.* **2005**, *39*, 9370–9376.

56. Morikawa, S.; Mabuchi, Y.; Kubota, Y.; Nagai, Y.; Niibe, K.; Hiratsu, E.; Suzuki, S.; Miyauchi-Hara, C.; Nagoshi, N.; Sunabori, T.; *et al.* Prospective Identification, Isolation, and Systemic Transplantation of Multipotent Mesenchymal Stem Cells in Murine Bone Marrow. *J. Exp. Med.* **2009**, *206*, 2483–2496.

57. Frank, O.; Heim, M.; Jakob, M.; Barbero, A.; Schäfer, D.; Bendik, I.; Dick, W.; Heberer, M.; Martin, I. Real-Time Quantitative RT-PCR Analysis of Human Bone Marrow Stromal Cells during Osteogenic Differentiation *in Vitro*. *J. Cell. Biochem.* **2002**, *85*, 737–746.

58. Eruslanov, E.; Kusmartsev, S. Identification of ROS Using Oxidized DCFDA and Flow-Cytometry. *Methods Mol. Biol.* **2010**, *594*, 57–72.